Supplementary Information (SI) for Soft Matter.

Supplementary Material for Linking structural and rheological memory in disordered soft materials

Krutarth M. Kamani,[1] Yul Hui Shim,[1] James Griebler,[1] Suresh Narayanan,[2] Qingteng Zhang,[2] Robert L. Leheny,[3] James L. Harden,[4] , Alexander Deptula,[5] Rosa M. Espinosa-Marzal,[6] Simon A. Rogers[1*]

[1]Department of Chemical and Biomolecular Engineering, University of Illinois at Urbana-Champaign, Illinois, USA 61801
[2]Advanced Photon Source, Argonne National Laboratory, Argonne, IL 60439, USA
[3]Department of Physics and Astronomy, Johns Hopkins University, Baltimore, MD 21218, USA
[4]Department of Physics, University of Ottawa, Ottawa, ON K1N 6N5, Canada
[5]Department of Materials Science and Engineering, University of Illinois at Urbana-Champaign, Illinois, USA 61801
[6]Department of Civil and Environmental Engineering, University of Illinois at Urbana-Champaign, Illinois, USA 61801
[*]To whom correspondence should be addressed; E-mail: sarogers@illinois.edu.

December 30, 2024

1 Relative memory

In addition to the absolute memory given by eq. 4, we can also define the *relative* memory of the material over the time interval $[t_1, t_2]$, $M_{rel}(t_1, t_2)$ as the change in the ultimate recoverable strain relative to the change in the total strain over the same interval,

$$M_{rel}(t_1, t_2) \equiv \frac{\int_{t_1}^{t_2} \dot{\gamma}_{rec} dt}{\int_{t_1}^{t_2} \dot{\gamma} dt} = \frac{\gamma_{rec}(t_2) - \gamma_{rec}(t_1)}{\gamma(t_2) - \gamma(t_1)}. \quad (1)$$

From this definition, it can be seen that the relative memory is unitless and is invariant with respect to an inversion of the interval, $M_{rel}(t_1,t_2) = M_{rel}(t_2,t_1)$.

The relative memory for simple step strain applied to a Hookean solid, in which all of the strain is acquired recoverably, $\gamma = \gamma_{rec}$, is one, $M_{rel} = \frac{\gamma_{rec}}{\gamma} = 1$. That is, the absolute memory says the system has an absolute memory of γ, which the relative memory says is all the strain that has been applied to it. For a Newtonian fluid that only ever acquires strain unrecoverably, both its absolute and relative memories are zero.

For cyclic experiments on an arbitrary material, two special cases can arise where the changes in recoverable and total strains over some interval are equal to zero. When the system is returned to a state of the same recoverable strain, the absolute and relative memories are both zero, while when the system is returned to a state where the total strain is the same, the relative memory will be undefined. For the case of a steady shear startup, where a constant shear rate is applied, the total strain increases as a function of time, starting from zero. The relative memory is always well defined in this protocol.

2 Beamline details, Material preparation, preshear protocol, offline rheological measurements

Beamline details: The x-ray incident beam on the sample has a size of $15\mu m$ x $15\mu m$, and the sample to detector distance is 7800 mm. The detector comprises of a 516 x 1556 array with pixel size of $55\mu m$ x $55\mu m$. The rheometer geometry was arranged with the Couette measurement cell axis oriented vertically, and the incident beam was directed radially through the center of the cell. This arrangement ensured that the incident beam was parallel to the shear-gradient (Δ) direction, enabling the collection of small-angle scattering in the flow-vorticity ($v - \omega$) plane.

Material preparation: The fumed silica colloidal suspension used in this study was prepared as in[1–4] by dispersing $2.9vol\%$ of hydrophobic fumed silica (R972, Evonik) in highly refined paraffin oil (18512, Sigma-Aldrich) and large molecular weight polyisobutylene (H25, Indopol), with the ratio between them $69wt\% : 31wt\%$. This was achieved using a Thinky mixer running at 2000 rpm for 1 hr.

Preshear protocol: Before performing any measurements, the material was presheared with an oscillatory strain amplitude of 100% at a frequency of 1 rps, in a nonlinear regime, followed by a period of zero stress and zero shear rate for 94 sec and 427 sec, respectively. The zero-stress step eliminates any directional bias while the zero shear rate step allows for the rebuilding of the isotropic structure.

Offline rheological measurements-recovery test: An iterative constrained recovery test was performed at 34 evenly spaced instants (see[5,6] for a detailed experimental protocol), using an MCR 302e rheometer from Anton Paar, at $22^{\circ}C$ using a cone and plate geometry with a diameter of 25 mm and a cone angle of 4°. A schematic of the oscillatory shear recovery test protocol is shown in Fig. S1. The protocol involves distinct steps that are iterated to form a complete set: 1) apply a sinusoidal strain to

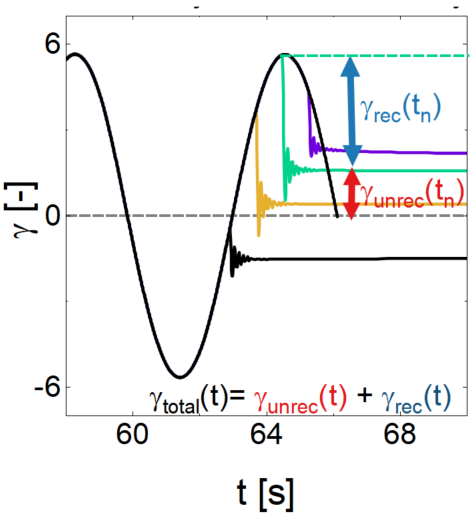

Figure 1 Schematic of oscillatory shear/recovery protocol at 1 rad/s.

reach steady alternance; 2) continue the oscillatory strain for a fraction of a period; and 3) apply zero shear stress to allow the material to recover to its ground state. This procedure was carried out in both forward and reverse directions and the average result was used to eliminate potential directional artifacts. For each set of measurements in forward and reverse directions, the preshear step was included to bring the material to the same ground state. This test provides three measured values for each time t_n: the total strain $\gamma_{total}(t_n)$; the unrecoverable strain (γ_{unrec}), which is the strain reached at the end of step 3; and the ultimate recoverable strain, $\gamma_{rec}(t_n)$. The sum of the components is equal to the total strain, so that $\gamma_{total} = \gamma_{rec} + \gamma_{unrec}$.

3 Obtaining rheological memory for the KDR model results

The model predictions were obtained numerically using MATLAB's ode15s solver. The following equations were solved as a system to determine recoverable strain for the strain-imposed oscillatory shear:

$$\sigma + \lambda(\dot{\gamma})\dot{\sigma} = (\eta_f)\left(\dot{\gamma} + \frac{\eta_s}{G}\ddot{\gamma}\right), \tag{2}$$

$$\sigma = G\gamma_{rec} + \eta_s\dot{\gamma}_{rec}. \tag{3}$$

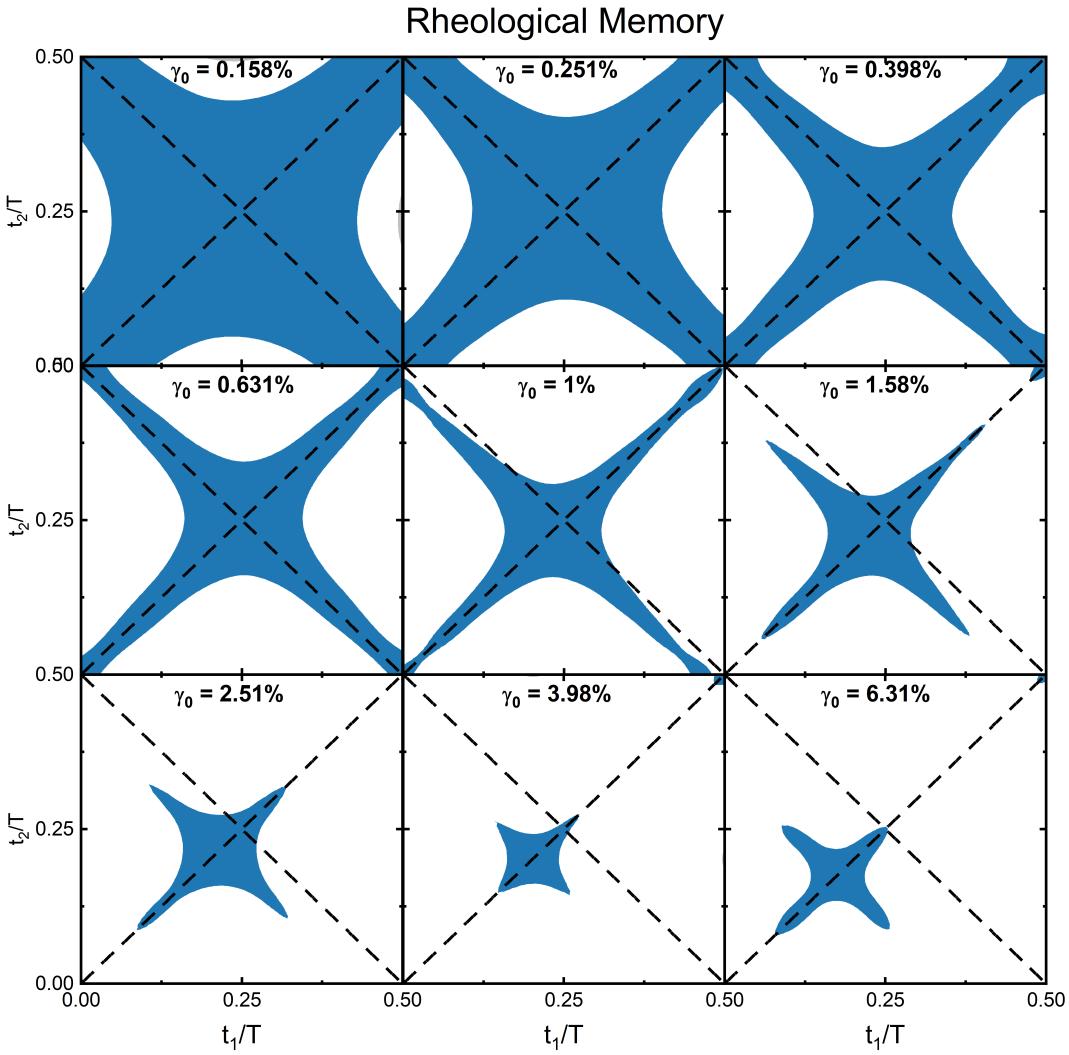

Figure 2 The absolute rheological memory of the fumed silica, for oscillatory shear at various strain amplitudes and at $\omega = 1$rad/s. The regions with blue color indicate zero absolute rheological memory.

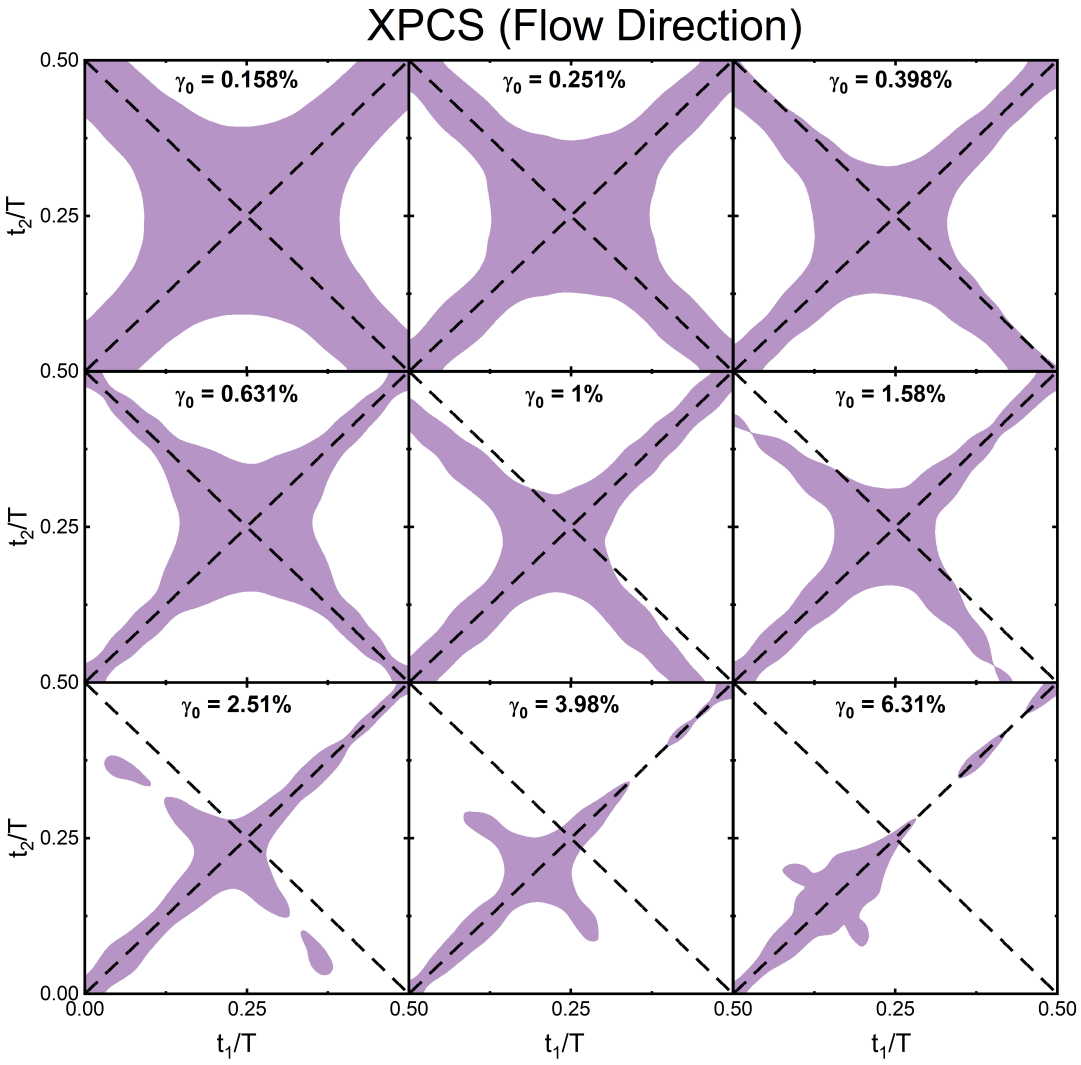

Figure 3 The XPCS two-time correlation function in flow direction for the fumed silica, for oscillatory shear at various strain amplitudes and at $\omega = 1\text{rad/s}$

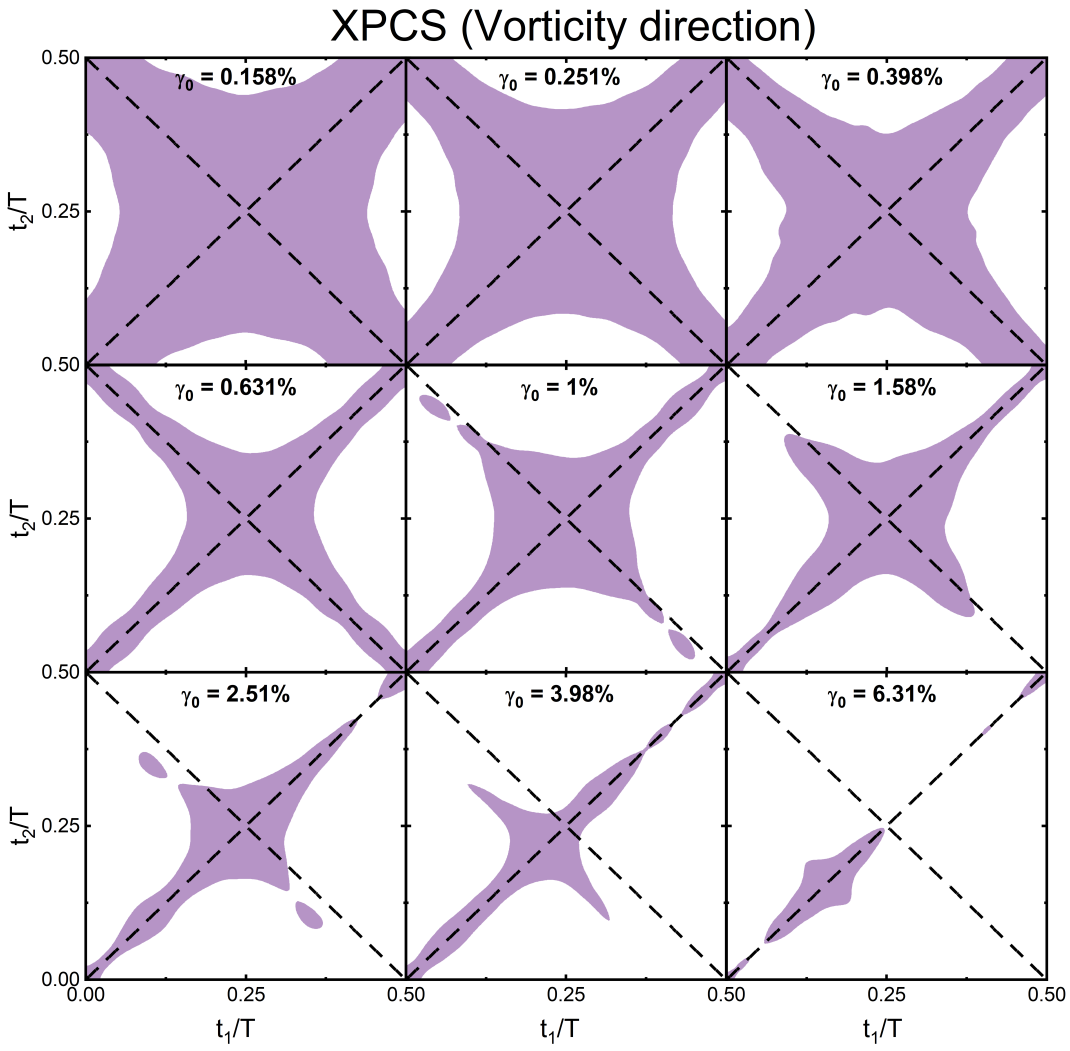

Figure 4 The XPCS two-time correlation function in the vorticity direction for the fumed silica, for oscillatory shear at various strain amplitudes and at $\omega = 1\text{rad/s}$

4 Variation of the rheological memory and XPCS correlation function at various strain amplitudes

In Figs. S2 and S3, we show the patterns exhibited by the rheological memory function, $\overline{M}_{abs}(t_1,t_2)$, and the XPCS correlation functions across a range of strain amplitudes from small to large. The colored region in Fig. S2 for the rheological memory indicates intervals with the same recoverable strain values and hence zero memory. The two-time correlation function obtained through XPCS measurements shows the correlation in microstructure whenever the rheological memory function is close to zero. As the strain amplitude varies from small to large, eliciting first linear and then non-linear responses, the age diagonal at which rheological memory is zero and structural recorrelation is observed in XPCS measurements shifts from a normalized age of $t_{age}/T = 0.25$ to $t_{age}/T = 0.15$. A smooth transition is observed for both patterns.

In Fig. S3, we show the variation of the XPCS correlation function in the vorticity direction, across a range of strain amplitudes from small to large. As can be observed, the same qualitative behavior is observed as was seen in the flow direction. As the strain amplitude varies from small to large, the age diagonal at which structural recorrelation is observed shifts to smaller values of t_{age}/T.

In Fig. 2(b) of the main manuscript, we show the two-time correlation plot from oscillatory shear at a small strain amplitude of 0.1%. For completeness, We show in Fig. S5 the two-time correlation plot for a large strain amplitude of 6.31%. The highest observed correlation value drops for large strain amplitude as compared to small strain amplitude. This is due to the fact that a part of the total strain is acquired unrecoverable.

5 Relation of XPCS correlation function during a single period of oscillation to quiescent state

As shown in Fig. 2 (b) of the main manuscript, before applying the desired oscillatory shear conditions, a zero strain rate step was included. This allows us to correlate the microstructure at any time during the oscillatory test to the initial quiescent nanostructure. In Fig. S6, for various strain amplitudes, we show that the correlation observed during a cycle is with respect to the microstructure present initially. Initially, for each strain amplitude, the high value of the XPCS correlation function corresponds to the quiescent state, as indicated by correlation value $C(t_1,-0.5s)$. As we apply oscillations at $t/T = 0$, the correlation value starts to drop, with its maxima reaching a constant value at the steady state. At all strain amplitudes, during the oscillation, we see some structural correlation with the initial microstructure present during the quiescent state. The Fourier-Transform analysis, shown in the inset, was used to convert the time domain response of the correlation value into the frequency domain.

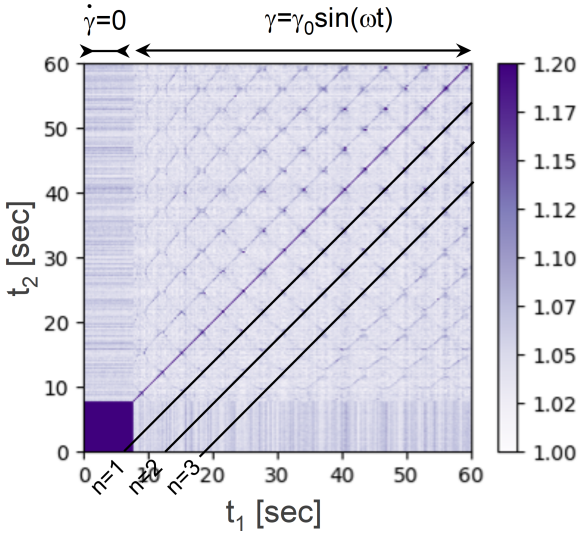

Figure 5 The XPCS two-time correlation plot from oscillatory shear at a large strain amplitude of 6.31% and at $\omega = 1$rad/s. The black lines parallel to $t_1 = t_2$ diagonal show the average of correlation function $C(t_1, t_1 - n2\pi)$ over multiple oscillation periods, indicated by n.

6 Variation of the rheological memory and XPCS correlation function for constant applied shear rate

In the main manuscript, we present the results for oscillatory shear to form a strong connection with prior literature. However, the proposed rheological memory function that links the bulk rheology to the microstructure is generic, as it can be equally applied under any deformation protocol. We show this by presenting the results for a steady shear startup experiment in Fig. S7. The protocol includes the application of $0.01s^{-1}$ for 1 sec followed by the application of the same shear rate in the reverse direction for $1.7s$. The yellow contour in Fig. S7 (a) shows the region with zero rheological memory (a change of less than 12 % in the recoverable strain value). When the shear rate is applied in the forward direction, some of the strain is acquired recoverably, eliciting an elastic-solid like response. As the direction of the shear is reversed, for the initial $1sec$, the strain acquired recoverably during the first step is recovered. Therefore, an age diagonal at the age of $t_{age} = 1$ sec is observed for the rheological memory. The corresponding XPCS measurement shows the microscopic structural correlation matches the bulk rheological memory function. This indicates that whenever the recoverable strain is the same, the microstructure is correlated.

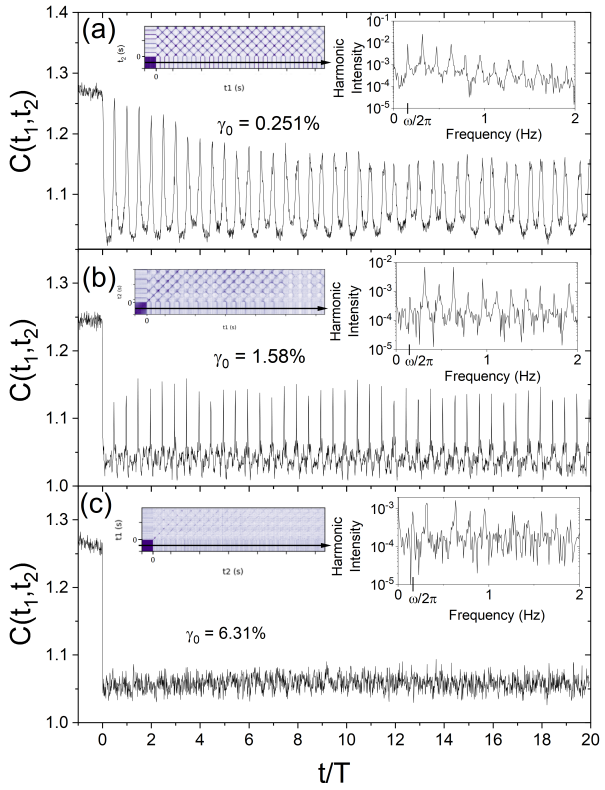

Figure 6 The relation of XPCS two-time correlation function $C(t_1, 3s)$ in the flow direction to the quiescent state at various strain amplitudes of 0.251%, 1.58%, 6.31%. The oscillations start at time 0 sec. The correlation value for $t < 0$ indicates the quiescent state. The inset shows the Fourier-Transform analysis of the time domain signal. The black arrow in the two-time XPCS correlation plot shows the line along which the correlation values are taken.

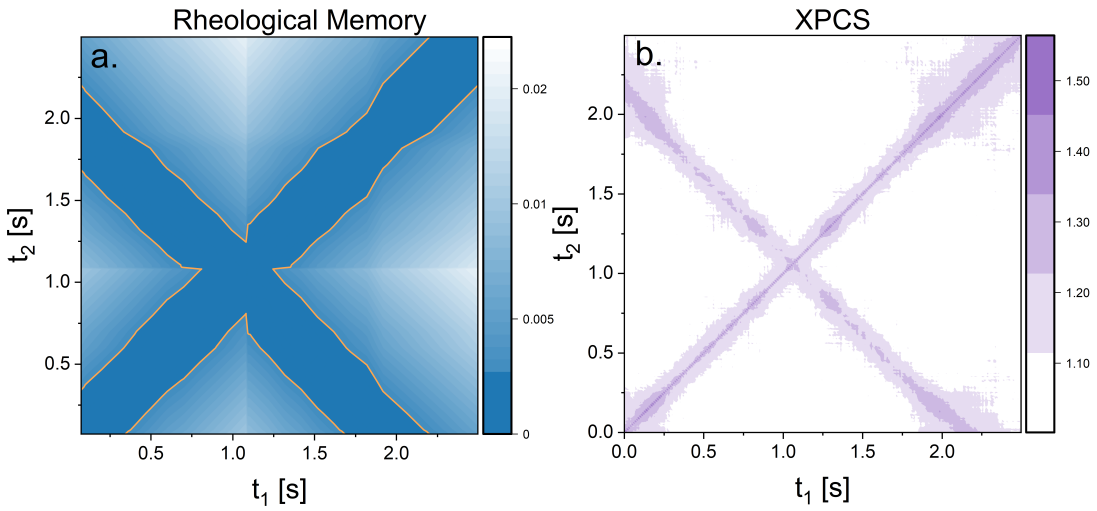

Figure 7 Comparison of the rheological memory and XPCS correlation function for the fumed silica sample, for steady shear startup tests at an applied shear rate of $0.01s^{-1}$.

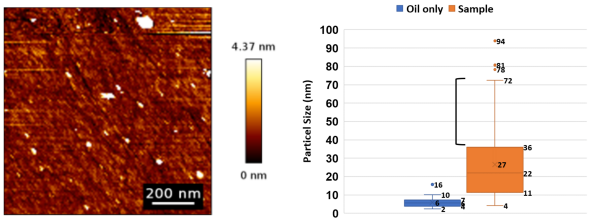

Figure 8 AFM-measurements: (a) Height map of fumed silica sample. Vertical color bar represents height in nm. (b) The box plot showing the particle size distribution.

7 Atomic force microscopy (AFM) measurements for determining the size of fumed silica particles

An atomic force microscope (Nano Wizard, JPK Instruments, Germany) was used for Quantitative Imaging (QI) of fumed silica particles adsorbed onto a PEI coated silicon wafer from a spin-coated sample. Additional oil solvent (mixture of paraffin oil (18512, Sigma-Aldrich) and polyisobutylene (H25, Indopol), with the ratio of $69wt\% : 31wt\%$) was added to completely immerse the AFM head. Sharp tips for QI imaging were Si tips with a nominal radius of 8 nm (HQ:CSC37/No Al, MikroMash, nominal spring constant 0.6-1.2 N/m). As shown in Fig. S8, topological line scans were extracted from images to determine the particle sizes. Due to the irregularity of fumed silica particles, the maxima of the profiles were used as an approximate value of particle diameter. The particle size of the fumed silica colloidal suspension varied from 11 nm to 36 nm. As shown in Fig. S9, the wave vector probed during the rheo-XPCS experiment ranges from

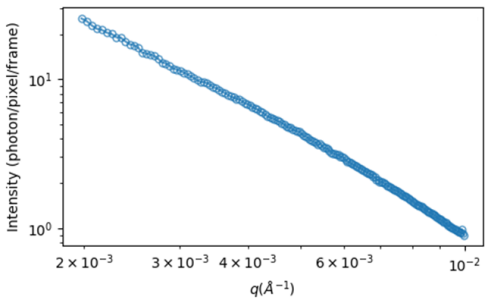

Figure 9 Rheo-XPCS intensity of the fumed silica colloidal suspension.

0.002 Å^{-1} to 0.01 Å^{-1}, which corresponds to the particle length scale in our colloidal fumed silica sample.

8 The raw absolute rheological memory for experiments and the KDR model

For completeness, in Figs. S10 and S11, we show the patterns exhibited by the rheological memory function, $\overline{M}_{abs}(t_1,t_2)$, for experiments and the KDR model, without any threshold. The regions inside the orange boundary indicate intervals with the same recoverable strain values and hence zero memory. The regions outside the orange boundary indicate regions with rheological memory greater than zero, $\overline{M}_{abs}(t_1,t_2) > 0$, with its magnitude being highest for the white regions.

Notes and references

[1] K. Dullaert and J. Mewis, *Rheologica Acta*, 2005, **45**, 23–32.

[2] Y. Wei, M. J. Solomon and R. G. Larson, *Journal of Rheology*, 2016, **60**, 1301.

[3] J. Choi and S. A. Rogers, *Rheologica Acta*, 2020, **59**, 921–934.

[4] M. Mahmoudabadbozchelou, K. M. Kamani, S. A. Rogers and S. Jamali, *Proceedings of the National Academy of Sciences*, 2022, **119**, e2202234119.

[5] J. C. W. Lee, K. M. Weigandt, E. G. Kelley and S. A. Rogers, *Phys. Rev. Lett.*, 2019, **122**, 1–6.

[6] G. J. Donley, P. K. Singh, A. Shetty and S. A. Rogers, *Proc. Natl. Acad. Sci. U.S.A.*, 2020, **117**, 21945–21952.

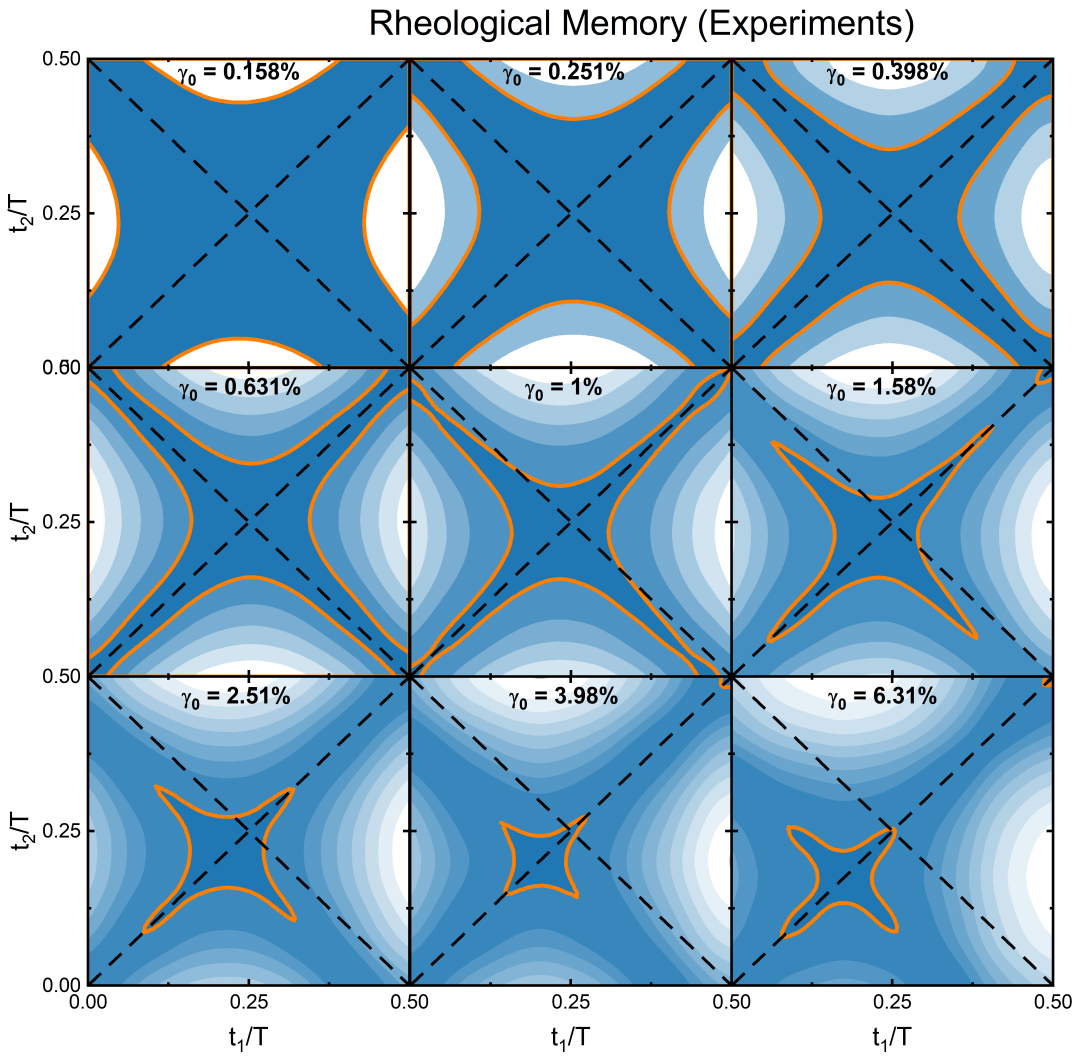

Figure 10 The full absolute rheological memory of the fumed silica, for oscillatory shear at various strain amplitudes and at $\omega = 1$rad/s. The regions within the orange color boundary indicate zero absolute rheological memory.

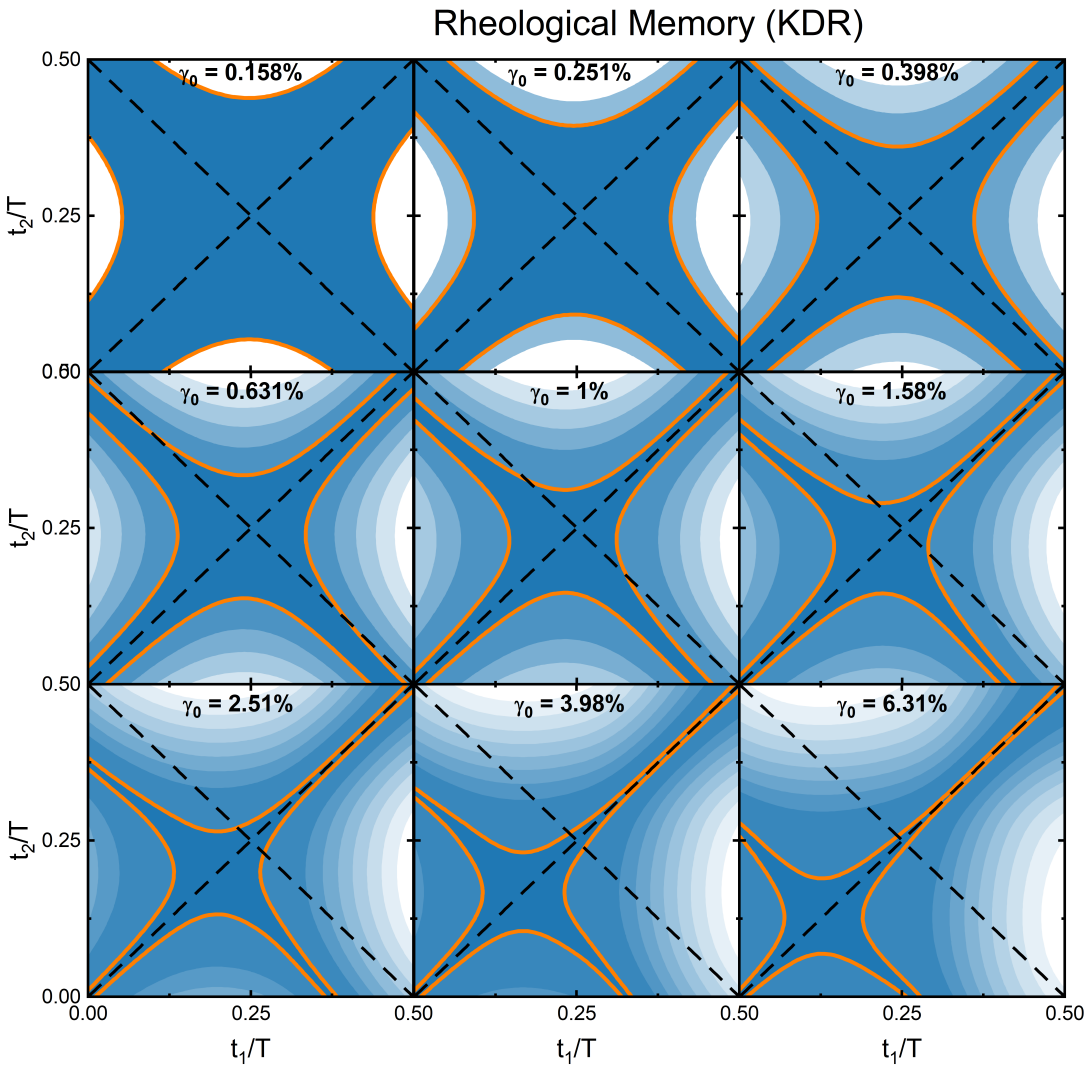

Figure 11 The full absolute rheological memory of the fumed silica, for oscillatory shear at various strain amplitudes and at $\omega = 1\text{rad/s}$. The regions within the orange color boundary indicate zero absolute rheological memory.